Capturing properties of three-fold coordinated silicon atom in silicon nitride: a positive correlation energy model

© *V.A. Gritsenko, Yu.N. Novikov, A.V. Shaposhnikov, Hei Wong*∗*, G.M. Zhidomirov*∗∗

Institute of Semiconductor Physics Siberian Branch of Russian Academy of Sciences,
630090 Novosibirsk, Russia
E-mail: grits@isp.nsc.ru

∗ Department of Electronic Engineering, Hong Kong, China
∗∗ Institute of Catalysis Siberian Branch of Russian Academy of Sciences,
630090 Novosibirsk, Russia

Electronic structure and capturing properties of three-fold coordinated silicon atom ($\equiv$ Si·) and the Si–Si bond in silicon nitride (Si_3N_4) were studied using the *ab initio* density functional theory. The results show that the previously proposed negative correlation energy (NCE) model is not applicable to Si_3N_4. The NCE model was proposed for interpreting the absence of the ESR signal for three-fold coordinated silicon defects and suggested that an electron can transfer between two silicon defects. We proposed that the absence of this ESR signal is due to the creation of neutral diamagnetic Si–Si defects in Si_3N_4. This model offers the most fundamental theory for explaining the hole localization (memory) effect in silicon nitride.

Carrier capturing in localized states or localization of electrons or holes is a fundamental process that governs the electronic properties of many amorphous solids, such as amorphous silicon, amorphous chalcogenides (*a*-Se, *a*-As_2S_3) and silicon nitride (Si_4N_4) films [1–4]. Particularly, amorphous Si_3N_4 is the most common material for observing this phenomenon as it has a gigantic cross–section (5×10^{-13} cm) for carrier capturing. An electron or a hole, being injected into the Si_3N_4 film, can be captured by a deep trap with a lifetime in the localized state of more than 10 years at room temperature [4]. This localization property is treated as memory effect from the application point of view. Its practical application is the use of amorphous Si_3N_4 as a gate dielectric in the SONOS (silicon-oxide-nitride-oxide-semiconductor) field effect transistors. Although this memory effect has been discovered for more than thirty years and is widely used in modern silicon devices [2,4–8], the exact nature and the kind of defects responsible for the carrier localization in the nitride film is still controversial. However, we already had a consensus that the localization of electrons and holes in the Si_3N_4 film is related to the intrinsic defects created by the excess silicon atoms [2,4,8,9].

The intrinsic defects in amorphous solids are believed to be due to the dangling bonds. However, most of the defects could not be detected with the electron spin resonance (ESR) measurement in a number of amorphous semiconductors and wide–gap polar dielectrics such as amorphous SiO_2 and Si_3N_4 films [1–4,10]. The signal for N_3Si· defect in silicon nitride, a three-fold coordinated silicon atom with unpaired electron, could be detected with ESR only after ultraviolet irradiation [11]. For freshly synthesized nitride film, no related ESR signal can be detected. This observation was explained with the negative correlation energy (NCE) model [12,13]. This model suggested that two diamagnetic defects: a positively charged N_3Si^+ and a negatively charged N_3Si^-:, can be formed from a N_3Si· (paramagnetic neutral defects in Si_3N_4) pair via the following reaction,

$$N_3Si· + ·SiN_3 \rightarrow N_3Si^+ : + : {}^-SiN_3. \tag{1}$$
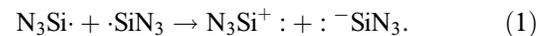
In the NCE model, the repulsive energy (U_C) of the two electrons localized in the Si atom is over-compensated by the energy gain in lattice relaxation with energy of U_L and the efective correlation energy $U = U_C + U_L$ becomes negative. According to the NCE model, reaction (1) is energetically favorable in the NCE model and the charged diamagnetic defects (N_3Si^+ and N_3Si^-:) are electron and hole traps which are supposed to be responsible for the memory effect in silicon nitride [2,8,14–17]. Latest *ab initio* density functional theory (DFT) calculations [18] showed that the correlation energy for N_3Si· defects is equal to 0.1 eV and the distance between two N_3Si· defects was about 3.1 Å. Hence the silicon dangling bonds can exchange electrons and the coulomb interaction at this distance is strong. However, experiments [4,19,20] showed that the electron trap density (N_t^e) and hole trap density (N_t^h) in Si_3N_4 are almost the same and are about 5×10^{18} cm^{-3}. The mean distance (a) between two traps in Si_3N_4 can be estimated by $a \approx (N_t)^{-1/3}$ and is about 60 Å which much larger than that used in the *ab initio* DFT calculation conducted by Pacchioni and Erbetta [18]. At the distance estimated from the experimental trap density, the Coulomb interaction is too week to make the electron exchange between two N_3Si· defects happening. This data suggests that the defect distribution is highly localized within a tetrahedral or between adjacent tetrahedral of the network. In addition, if the distance between two defects is about 3.1 Å, other mechanisms for the carrier localization are also possible. It was suggested that the electron and hole capturing could also occur at a neutral diamagnetic $\equiv$ Si−Si $\equiv$ defect [2,4,10,20,21]. The validity

a

● Si

◐ N

○ H

b

c
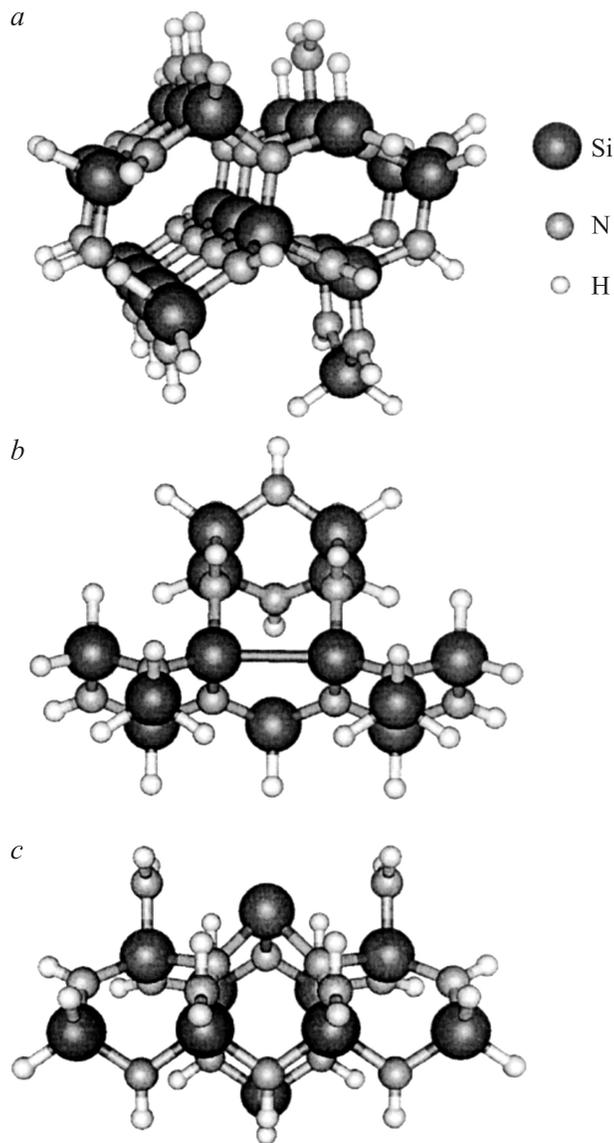
Fig. 1. Cluster models used in the simulation. (*a*) the 84-atom cluster for bulk nitride simulation, (*b*) the 56-atom cluster for the Si–Si bond simulation and (*c*) the 55-atom cluster for the ≡ Si· defect simulation.

of these two models for Si_3N_4 is still under discussion. This paper aims to validate the NCE model and the Si–Si bond model in silicon nitride by using the quantum-chemical DFT simulation. Quantum chemical simulation was successfully used for studying the electronic structures of the defects in silicon oxide and electronic properties of other defects in Si_3N_4 films [18,22–25].

The simulations were conducted on the $N_3Si\cdot$ and $N_3Si–SiN_3$ defects created from the fragments of crystalline β-Si_3N_4. Fig. 1 shows three clusters used for the simulation. The 84-atom cluster ($Si_{20}N_{28}H_{36}$) with hydrogen-passivated sufrace (Fig. 1,*a*) was used for simulating the bulk electronic structure of Si_3N_4 and for estimating the energy gain for the carrier capturing. The 56-atom cluster $Si_{14}N_{12}H_{30}$ (shown in Fig. 1,*b*) was used for simulating

the capturing properties of the $N_3Si–SiN_3$ defect. The 55-atom $Si_{10}N_{18}H_{27}$ cluster shown in Fig. 1,*c* was used for simulating the properties of the $N_3Si\cdot$ defect. Geometric relaxation of the Si atoms at different charged states was allowed during the simulation.

We performed *ab initio* DFT calculations using the ADF program [26] where the exchange–and–correlation (XC) functional consists of the generalized gradient approximation (GGA) part: GGA–XC. The Kohn–Sham molecular orbits were constructed using the Slater-type exponential basis functions and the basis set includes the doublezeta basis with the polarization function for all atoms (i. e. the basis set III in ADF terminology). All electrons were included in valence basis. In addition, the positions of all Si and N atoms were fully optimized at the non-local DFT level using the Becke form [27] of exchange and the Lee–Yang–Parr theory [28].

The energy gains for capturing an electron (ΔE^e) and a hole (ΔE^h) were calculated using the formula

$$\Delta E^e = \left(E_{bulk}^- + E_{defect}^0\right) - \left(E_{bulk}^0 + E_{defect}^-\right), \qquad (2)$$

$$\Delta E^h = \left(E_{bulk}^+ + E_{defect}^0\right) - \left(E_{bulk}^0 + E_{defect}^+\right), \qquad (3)$$

where E_{bulk}^0, E_{bulk}^-, and E_{bulk}^+ are the total energies of the „bulk" clusters for Si_3N_4 in neutral, negative and positive charge states, respectively, and E_{defect}^0, E_{defect}^-, and E_{defect}^+ are the total energies for the defect clusters in neutral, negative and positive charge states, respectively. If the value of the energy gain is positive, then capturing of an electron or a hole from the bulk of Si_3N_4 by the $N_3Si\cdot$ or $N_3Si–SiN_3$ defect will result in the release of energy.

The $N_3Si\cdot$ defect was discussed intensively in the literature as a defect responsible for the carrier localization in Si_3N_4 films [4,8,9,18,29–31]. In agreement with Pacchion and Erbetta [18], our calculations show that the $N_3Si\cdot$ defect can be a trap for electrons. However, our result show that the $N_3Si\cdot$ defect cannot capture a hole as this process is energetically unfavorable. This result was also obtained previously by Pacchion and Erbetta [18]. However, the absence of the paramagnetic signal in a virgin Si_3N_4 film indicates that the $N_3Si\cdot$ defect should not be responsible for the memory effect [2,10].

To ensure the cluster model be reliable enough for simulating the electronic structure of silicon nitride, we simulated the *X*-ray emission spectra of bulk Si_3N_4. The calculations were performed in the frozen orbital approximation. Dipole matrix elements were calculated between core (Si $1s$, $2p$ and N $1s$) orbits and valence orbits. These matrix elements include, in principle, all inter-atomic matrix elements between the Slater-typer functions centered on different atoms. The calculated spectra were then broadened by convoluting the Lorentz curves with a width of 0.5 eV. We found that the Si $3d$ polarization functions must be included in the basis set in order to obtain a Si *L X*-ray emission spectrum in agreement with the experimental results. Our calculation also shows that the contributions of Si *K* and N *K* emission spectra in to the non-local
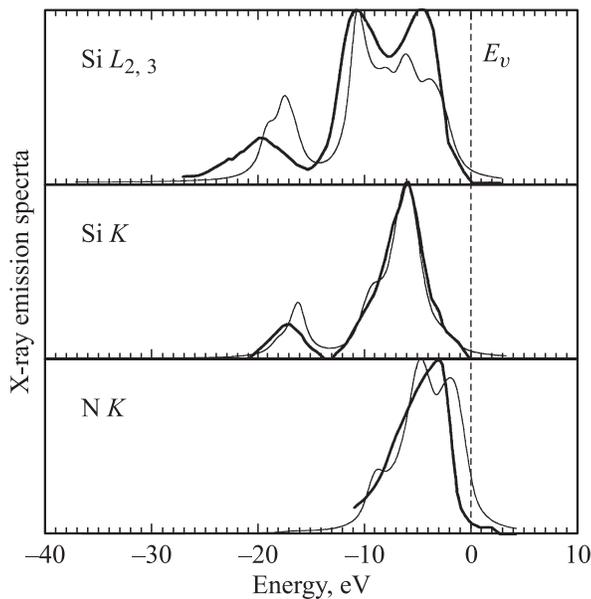
Fig. 2. *X*-ray emission spectra of silicon nitride calculated using the DFT theory (thin lines). Experimental results [4] are also shown for comparison (thick lines).

transitions are negligible. Fig. 2 shows our calculation results. Previous experimental results of Si *K*, Si *L* and N *K* spectra [4] are also shown for comparison. In general, a good agreement between the calculated and the experimental data is observed. The simulation results show that the main contributions to the valence band of silicon nitride are from N $2p$, Si $3s$, $3p$ and $3d$ orbits.

To verify the NCE model, we calculated the total energies of the 55-atom cluster with the three-fold coordinated silicon atom in the three different charge states: $N_3Si\cdot$, N_3Si^+, and N_3Si^-: using the DFT method. To estimate the long-range order lattice polarization during the charge trapping, we used the simplest approach based on the classical Born model [18]. According to this model, the long-range polarization will reduce the cluster total energy of the defect by 0.7 eV. Our simulation shows that the total energy of the two neutral clusters with the $N_3Si\cdot$ defect is of 2.1 eV less than the total energies of the negatively charged N_3Si^- defect and the positively charged N_3Si^-: defects when the longrange polarization is taken into account. It indicates that the conversion of a pair of the neutral three-fold coordinated silicon atoms $N_3Si\cdot$ to a pair of the charged diamagnetic states (N_3Si^+, and N_3Si^-:) according to reaction (1) is energetically unfavorable. And the energy gain U_L from the lattice distortion cannot over-compensate the large coulomb repulsive energy U_C. Hence, the NCE model is not applicable to the carrier capturing of the three-fold coordinated silicon atoms in Si_3N_4. Instead, we proposed the formation of a neutral diamagnetic $\equiv Si-Si \equiv$ bond from the $\equiv Si\cdot$ defect pair with the positive correlation energy (PCE). The theory was proposed for the silicon defects ($Si_3Si\cdot$) in amorphous silicon [32,33] and the $O_3Si\cdot$ defect in SiO_2 films [34,35].

The Si–Si bond length in silicon is 2.35 Å and the silicon–silicon distance in Si_3N_4 is about 3.1 Å [2]. In order to estimate the Si–Si bond length in the $N_3Si-SiN_3$ defect, we performed DFT calculations at MP2/6, QCISD/6, and B3LYP/6 levels [26]. The $(NH_2)_3Si-Si(NH_2)_3$ cluster was used for the simulation. To calculate the energy change of the cluster when the Si–Si bond length deviates from the optimized bond length, we first fixed the N–H bond length and the angle of SiNH in the cluster. According to the simulation, the optimal Si–Si bond lenght is 2.35 Å which is the same as the Si–Si bond length in Si (see Fig. 3). To understand the charged state of a $(NH_2)_3Si-Si(NH_2)_3$ species, we calculated the Mulliken charge distribution on the two Si atoms of a $(NH_2)_3Si-Si(NH_2)_3$ cluster. Increase of Si–Si bond length is accompanied by the increase of total cluster energy and gives rise to the symmetric charge distribution in both of the Si atoms. Consequently, two paramagnetic $N_3Si\cdot$ species were created by breaking the Si–Si bond, i. e.,

$$N_3Si - SiN_3 \leftrightarrow N_3Si \cdot + \cdot SiN_3. \tag{4}$$
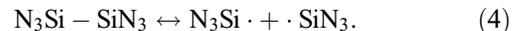
The symmetric charge distribution obtained in this work shows that the creation of two charged N_3Si^+, and N_3Si^-: defects at a distance in the range of 2–3 Å is energetically unfavorable. Instead, creation of diamagnetic symmetric Si–Si bond is more favorable.

To determine the most favorable state of the Si atoms, we analyzed the total energies of different clusters. The total energy of the $(NH_2)_3Si-Si(NH_2)_3$ cluster is 3.15 eV less than that of the two $(NH_2)_3Si\cdot$ defect and the total energies of N_3Si^+ and N_3Si^-: defects is 2.1 eV greater than that of the two $(NH_2)_3Si\cdot$ defects. Hence the most favorable one is the formation of neutral diamagnetic Si–Si bonds, neutral paramagnetic state $N_3Si\cdot$ less and the most unfavorable one is the formation of diamagnetic charged N_3Si^+ and N_3Si^-: states.
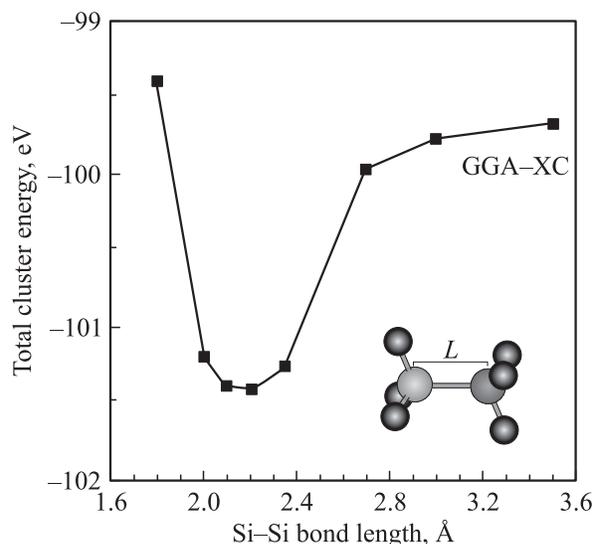
Fig. 3. Plot of the total energy of the $H_6N_3Si-SiN_3H_6$ cluster as a function of the Si–SI bond distance.

DFT calculation were also conducted for a Si–Si bond with a captured hole or electron using the 56-atom $Si_{10}N_{18}H_{27}$ cluster. Our DFT simulation shows that the Si–Si bond in Si_3N_4 can capture a hole. This result is similar to the SiO_2 case. The calculated energy gain for the hole captured on the Si–Si bond is about 1 eV. The hole capturing on a Si–Si bond plays an important role in silicon devices with oxynitride as the gate dielectric [36]. Si–Si bonds were observed experimentally at the Si_3N_4 / termal oxide interface [21]. Excess hole and electron capturings at the interface were also found [37,38].

The presence of Si–Si bonds naturally explains the absence of the ESR signal in the virgin Si_3N_4 film. The model also predicts that the Si–Si defect becomes paramagnetic after hole capturing. However, experiments showed that carrier capturing in Si_3N_4 cannot be detected with the ESR measurement [2,10]. Explanation for the absence of the ESR signal in Si_3N_4 with captured carriers was proposed [10,38]. This is due to the spin coupling of the hole localized by the Si–Si bond as a result of resonance tunneling via non–occupied traps [10,38]. In fact, both electron and hole localization were found in silicon nitride. Since the Si–Si bond can capture electron in amorphous silicon [32,33], one may suggest that the Si–Si bond in Si_3N_4 can also capture an electron. However, the DFT results do not predict the electron capturing by Si–Si bonds due to the negative energy gain. Thus, we have to find other possibility for electron capturing effect in silicon nitride. We suggested that the electron localization in Si_3N_4 is due to the two-fold coordinated nitrogen atom [39].

In conclusion, we belive that the creation of a pair of charged diamagnetic defects $\equiv Si^+$, and $\equiv Si^-$: from a neutral diamagnetic $\equiv Si\cdot$ defects pair with the negative correlation energy (NCE) is invalid in silicon nitride for the following reasons.

(1) New *at initio* DFT quantum-chemical simulation results suggest that hole capturing in the $N_3Si\cdot$ defect is energetically unfavorable.

(2) The energy gain U_L from the lattice distortion cannot over compensate the large Coulomb repulsive energy U_C in the NCE model.

With this connection, we proposed the formation of a neutral diamagnetic $\equiv Si-Si \equiv$ bond from the $\equiv Si\cdot$ defects pair with the PCE. Simulation shows that the $\equiv Si-Si \equiv$ bond in Si_3N_4 can capture holes. This model explains the memory effect in silicon nitride.

References

[1] N.F. Mott, E.A. Davis. Electronic Processes in Non–Crystalline Materials. Clarendon, Oxford (1979).
[2] W.L. Warren, J. Kanicki, J. Robertson, E.H. Poindexter, P.J. McWhorter. J. Appl. Phys. **74**, 4034 (1993).
[3] V.A. Gritsenko. Structure and Electronic Properties of Amorphous Dielectrics in Silicon MIS Structures. Science, Novosibirsk, Russia (1993).
[4] V.A. Gritsenko. In: Silicon Nitride in Electronics / Ed. by A.V. Rzhanov. Elsevier, N. Y. (1988).
[5] H. Bachofer, H. Reisinger, E. Bertagnolli, H. von Philipsborn. J. Appl. Phys. **89**, 2791 (2001).
[6] J. Bu, M.H. White. Solid State Electron. **45**, 113 (2001).
[7] B. Eitan, P. Pavan, I. Bloom, E. Alony, A. Frommer, D. Finzi. IEEE Electron Device Lett. **21**, 543 (2000).
[8] Y. Yang, M.H. White. Solid State Electron. **44**, 949 (2000).
[9] S. Fujita, A. Sasaki. J. Electrochem. Soc. **132**, 398 (1985).
[10] V.A. Gritsenko, A.D. Milov. JETP Lett. **64**, 531 (1996).
[11] W.L. Warren, P.M. Lenahan. Phys. Rev. B **42**, 1773 (1990).
[12] P.W. Anderson. Phys. Rev. Lett. **34**, 953 (1975).
[13] R.A. Street, N.F. Mott. Phys. Rev. Lett. **35**, 1293 (1975).
[14] J. Robertson. Appl. Phys. Lett. **44**, 415 (1984).
[15] E.E. Meerson, S.P. Sinitsa. Microelectron. **16**, 37 (1987).
[16] S.E. Gurri, P.M. Lenahan, D.T. Krick, J. Kanicki, C.T. Kirk. Appl. Phys. Lett. **56**, 1359 (1990).
[17] Y. Roizin, L. Tsibeskov. J. Non–Cryst. Solids **137&138**, 515 (1991).
[18] G. Pacchioni, D. Erbetta. Phys. Rev. B **61**, 15 005 (2000).
[19] V.A. Gritsinko, E.E. Meerson, I.V. Travkov, Yu.V. Goltviansky. Microelectron. **16**, 42 (1987).
[20] Y. Kamigaki, S. Minami, H. Kato. J. Appl. Phys. **68**, 2211 (1990).
[21] V.A. Gritsenko, H. Wong, J.B. Xu, R.M. Kwok, I.P. Petrenko, B.A. Zaizev, Yu.N. Morokov, Yu.N. Novikov. J. Appl. Phys. **86**, 3234 (1999).
[22] G. Pacchioni. Phys. Rev. Lett. **79**, 753 (1997).
[23] G. Pacchioni, G. Ierano, A.M. Marquez. Phys. Rev. Lett. **81**, 377 (1998).
[24] G. Pacchioni, D. Erbetta. Phys. Rev. B **60**, 12 617 (1999).
[25] C. Fonseca Guerra, J.G. Snijders, G. Te Velde, E.J. Baerends. Theor. Chem. Acc. **99**, 391 (1998).
[26] A.D. Becke. Phys. Rev. A **38**, 3098 (1988).
[27] C. Lee, W. Yang, R.G. Parr. Phys. Rev. B **37**, 785 (1988).
[28] J.K. Rudra, W.B. Fowler. Phys. Rev. B **35**, 8223 (1987).
[29] D.T. Krick, P.M. Lenahan, J. Kanicki. Phys. Rev. B **38**, 8226 (1988).
[30] J. Robertson. Philos. Mag. B **69**, 307 (1994).
[31] T. Umeda, S. Yamasaki, J. Isoya, A. Matsuda, K. Tanaka. Phys. Rev. Lett. **77**, 4600 (1996).
[32] T. Umeda, S. Yamasaki, J. Isoya, K. Tanaka. Phys. Rev. B **62**, 15 702 (2000).
[33] W.B. Fowler, J.K. Rudra, M.E. Zvanut, F.J. Feigle. Phys. Rev. B **41**, 8313 (1990).
[34] W.L. Warren, E.H. Poindexter, M. Offenberg, W. Muller–Warmuth. J. Electrochem. Soc. **139**, 872 (1992).
[35] V.A. Gritsenko, J.B. Xu, R.M. Kwok, Y.H. Ng, I.H. Wilson. Phys. Rev. Lett. **35**, 1293 (1998).
[36] E. Suzuki, Y. Hayashi, T. Tsuchiya. Appl. Phys. Lett. **42**, 6008 (1983).
[37] Z.A. Weinberg, K.J. Stein, T.N. Nguen, J.Y. Sun. Appl. Phys. Lett. **57**, 1248 (1990).
[38] V.A. Gritsenko. JETP Lett. **64**, 525 (1996).
[39] Yu.N. Morokov, Yu.N. Novikov, V.A. Gritsenko, H. Wong. Microelectron. Engineer. **48**, 175 (1999).